SPECIAL PROJECT PROGRESS REPORT

All the following mandatory information needs to be provided. The length should *reflect the complexity and duration* of the project.

Reporting year	2021
Project Title:	FLEXPART energy transport simulations and inverse modelling of atmospheric constituents
Computer Project Account:	spatvojt
Principal Investigator(s):	Martin Vojta
Affiliation:	University of Vienna – Institute of Meteorology and Geophysics
Name of ECMWF scientist(s) collaborating to the project (if applicable)	………………………………………………………….…… ………………………………………………………….……
Start date of the project:	2021
Expected end date:	2023

Computer resources allocated/used for the current year and the previous one

(if applicable)

Please answer for all project resources

		Previous year		Current year	
		Allocated	Used	Allocated	Used
High Performance Computing Facility	(units)			1000000	
Data storage capacity	(Gbytes)			10000	

Summary of project objectives (10 lines max)

The Lagrangian particle dispersion model FLEXPART (Stohl et al., 2005, Pisso et al., 2019) is run with ECMWF data to explore the dispersion and transport of various atmospheric constituents. The model is used with inversion techniques to enhance the knowledge about the emissions of several atmospheric compounds. This helps to get a better understanding of their impact on the Earth's climate system and air quality and to improve transport simulations of these substances. Furthermore, by performing domain-filling simulations the model is used to develop Lagrangian climatologies of heat and energy transport in the atmosphere and to perform case studies of extreme weather events.

Summary of problems encountered (10 lines max)

……………………………………………………………………………………………………

Summary of results

If submitted **during the first project year**, please summarise the results achieved during the period from the project start to June of the current year. A few paragraphs might be sufficient. If submitted **during the second project year**, this summary should be more detailed and cover the period from the project start. The length, at most 8 pages, should reflect the complexity of the project. Alternatively, it could be replaced by a short summary plus an existing scientific report on the project attached to this document. If submitted **during the third project year**, please summarise the results achieved during the period from July of the previous year to June of the current year. A few paragraphs might be sufficient.

1) Energy Export from the Tropical Pacific by using a Lagrangian re-analysis

By performing domain-filling transport model simulations with the Lagrangian particle dispersion model, as well as forward and backward simulations for particular sites, Lagrangian transport climatologies, as well as global statistics can be established. For an already existing Lagrangian re-analysis, the ERA-Interim dataset from ECMWF was used on a three-hourly basis. Therefore, five million particles were released at the first timestep, globally distributed and transported forward in time. These particles remain in the atmosphere over the whole time period and represent the atmospheric mass. The dataset ranges from 1990 to 2016 and consists of five million trajectories that are 26 years long. In addition, this FLEXPART-setup is adopted and currently running with the new ERA5 re-analysis dataset from ECMWF from 1970 on. As soon as this simulation is done, we will adopt all our analysis to it. However, results that are presented here, were calculated with the already existing dataset (ERA-Interim).

By using this Lagrangian re-analysis, the energy export from the Tropical Pacific can be detected. Therefore, only particles that have been within the Nino3.4 region and below 1 km were selected and followed forward in time. *Figure 1* shows that the transported air masses lose energy over the Atlantic, and gain energy over the West Pacific, at least for December 1997. This analysis is done for each month of the whole dataset and differences between El Niño and La Niña are detected. It can be seen (not shown here) that during an El Niño event more mass is transported eastward, while during La Niña more mass is transported westward.

By taking a deeper look into the moisture transport, we found that during La Niña more moisture is transported towards the West and especially South Asia, while during El Niño the air masses transported to the East are relatively dry. But more evaluations need to be done, especially with the new dataset that used the ERA5 data.

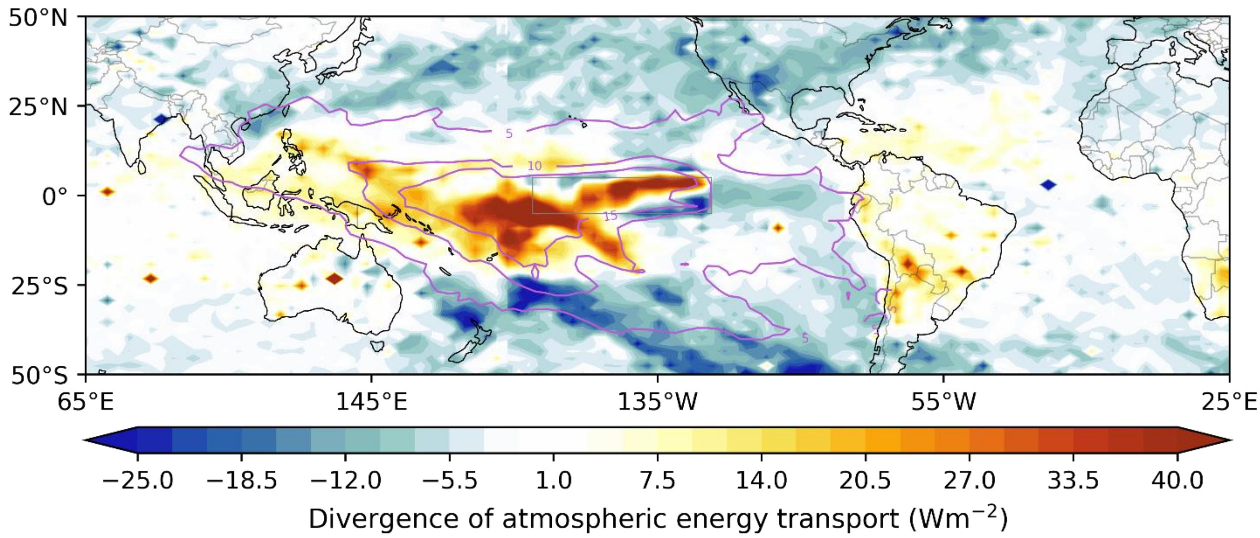

***Figure 1**: Energy export from particles that have passed the Nino3.4 box (5°S-5°N, 170°W-120°W, < 1km) within the past three weeks. Here the mean over December 1997 (strong El Niño case) is shown. The divergence of total energy is shown in colour, and the contour lines represent the fraction of the transported air mass from the Nino3.4 box relative to the total mass of the atmosphere.*

2) Inverse Modelling of Fluorinated Gases – Sensitivity to the Baseline Definition

When using Lagrangian models as basis for atmospheric inversions, one source of uncertainty is the definition of the baseline – a concentration that should account for all the flux contributions to the observed mixing ratios that are not covered in the inversion. We investigate three different, well established baseline methods to study their influence on inversion results, modelling sulfur hexafluoride (SF_6) for the year 2012. The REBS method introduced by Ruckstuhl et al. (2012) detects baseline observations by iteratively fitting a local linear regression model to the data, excluding data points outside a certain range around the baseline. A method introduced by Stohl et al. (2009) is also primaly based on the selection of observations, but in addition uses model information to determine the baseline. The global distribution-based method couples global fields of mixing ratios to the modelled backwards-trajectories at their point of termination. In this project, we used the hourly meteorological re-analysis dataset ERA5 from ECMWF for two purposes: (1) the Lagrangian particle dispersion model FLEXPART was driven with ERA5 to calculate the source-receptor relationship which the inversion is based on, and (2) ERA5 was used to perform a global re-analysis of SF_6 for the year 2012, since global fields of SF_6 mixing ratios were needed in order to apply the global distribution-based method.

We find that at stations located in areas with lots of pollution episodes the REBS method produces lower baselines than Stohl's method or the global distribution-based method – as illustrated in *Figure 2* for the observation station Hateruma (hat) in Japan. Consequently, the inversion calculates lower emissions in countries with many pollution events when applying the REBS method than when using the other two methods. The biggest differences can be found in China, where modelled emissions are almost 50% lower when using the REBS method compared to Stohl's method or the global distribution-based method (*Figure 3*).

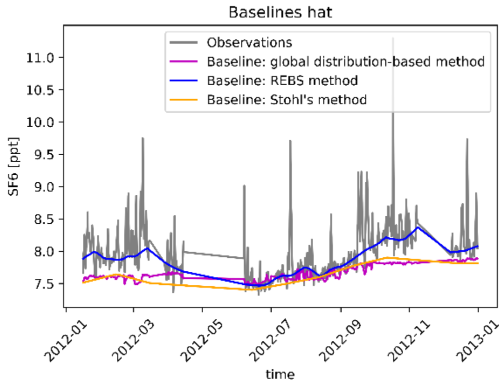

***Figure 2**: Baselines at hat observation station calculated with the global distribution based-method, REBS method and Stohl's method*

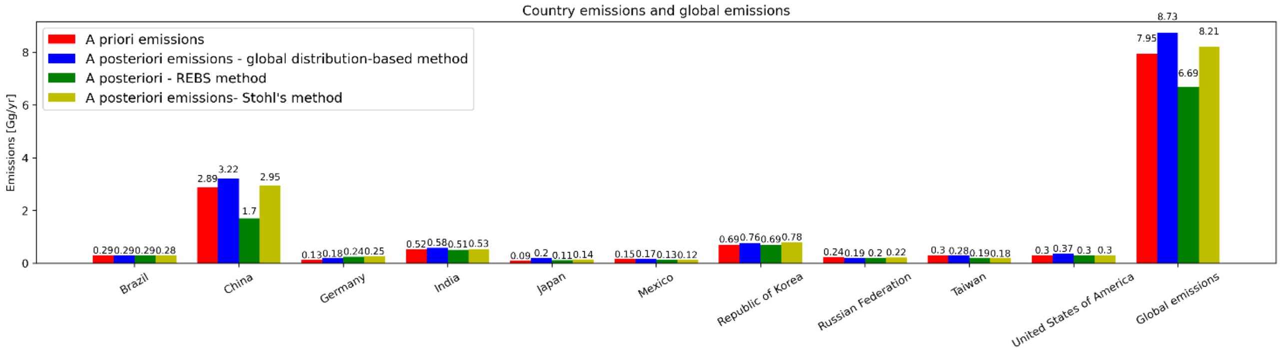

***Figure 3:** Calculated country emissions and global emissions of SF_6 for the year 2012 applying the global distribution based-method, REBS method and Stohl's method*

3) Emission sensitivities of ice core sites

We used the ERA5 re-analysis dataset to drive FLEXPART simulations for several collaborators who analyse deposition of various species in ice cores. For these simulations FLEXPART was run in backward mode following virtual air particles back in time starting from the individual ice core sites. Performing such simulations for several thousand particles results in a map of emission sensitivity for the specific site. As an example, *Figure 4* shows the emission sensitivities for two Antarctic ice cores sites (red dots), at Berkner Island (left) and at the South Pole (right). The plots indicate the deposition signal (in µg/m^2/a) an emission of unit strength (1 kg/s) would have on the respective site. In other words, the ice core locations are more sensitive to emissions from orange/yellow regions than they are to emissions from blue/violet regions. While Berkner Island is sensitive to a larger region, the South Pole is more isolated.

Besides Antarctic sites, we also performed simulations for Greenlandic and Alpine ice core sites. The simulated emissions sensitivities will be used to help with the interpretation of ice core measurements by identifying most likely source regions; which caused the observed depositions in the ice cores.

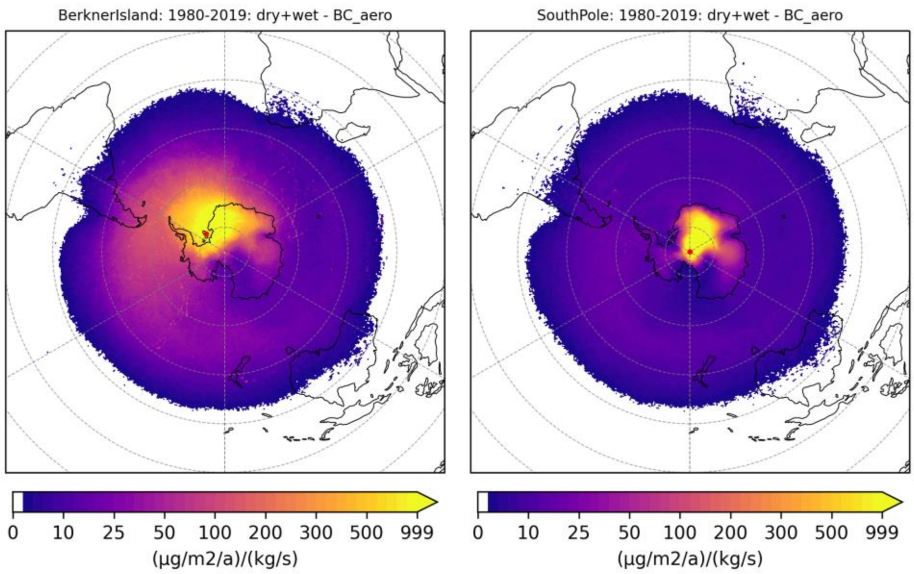

***Figure 4**: Emission sensitivities for two Antarctic ice core sites (red dots) – left: Berkner Island; right: South Pole; annual mean sensitivities for the period 1980 to 2019; simulated with FLEXPART v10.4 and ERA5 0.5° input*

4) Air masses origin for the MOSAIC artic campaign interpretation

The Multidisciplinary drifting Observatory for the Study of Arctic Climate (MOSAiC) ship expedition took place in the Arctic for a whole year, starting from September 2019, with the goal to improve the understanding of the atmospheric, oceanic and sea ice processes of the region affecting the arctic climate system. To support the interpretation of trace gas and aerosol as well as meteorological measurements collected by the ship, backward transport calculations were performed, along the whole duration of the campaign, with the Lagrangian particle dispersion model FLEXPART. FLEXPART was driven with hourly ERA5 data at 0.5° horizontal resolution. Every 3 hours, 100000 particles, representative of a generic passive tracer, were initialized at the ship location and traced backward for 30 days. The output, indicated here as footprint emission sensitivity (FES), represents the residence time of the trajectories in a layer close to the surface (< 100m a.g.l.).
The results, shown in *Figure 5*, indicate that interactions with ocean and sea ice surfaces were dominant year-round with very little interaction with the surface. The only significant interactions occurred over North Asia, mostly during winter and early spring. This is typical for the Arctic and explains the relatively lower concentrations of anthropogenic pollutants in summer than in winter (Stohl, 2006). Ice-covered surfaces were most influential in winter and early spring, when the sea ice extent was at its maximum. During late spring, while the sea ice was still covering a large part of the Arctic ocean, a considerable fraction of the air masses was transported from ice-free regions, and the relative contribution of the ocean in the time series increased accordingly. The highest influence from the ocean surface occurred in late summer and autumn. More in general, there was relatively less interaction with the near-surface environment in spring and summer compared to the rest of the year, most likely associated with a stronger descent of air masses in summer.

More detailed results from the FLEXPART output for the whole campaign (including different species, layers, and transport durations) can be found on the following website:
https://img.univie.ac.at/webdata/mosaic

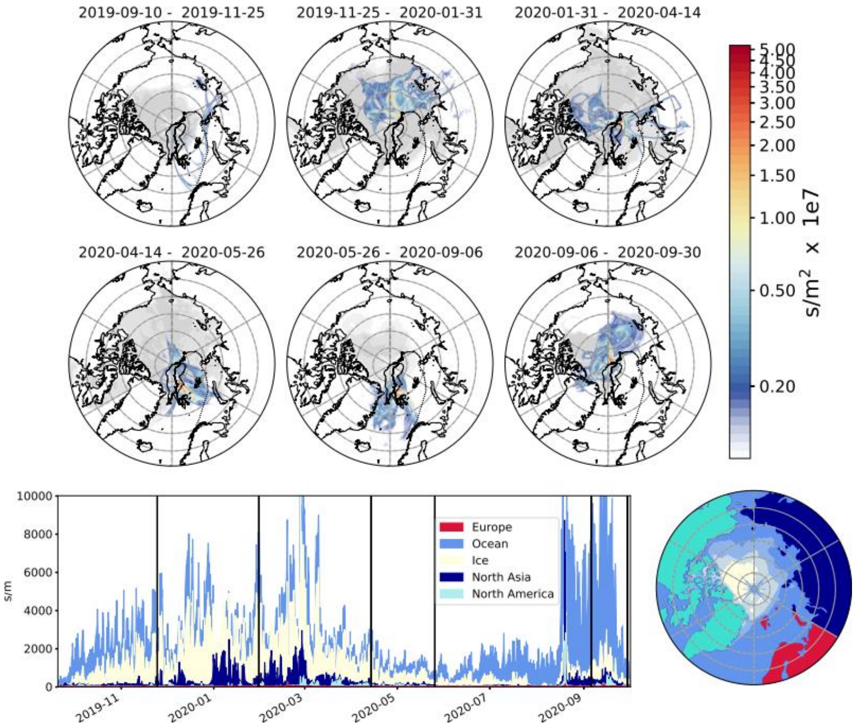

***Figure 5**: Top: Footprint emission sensitivity, per m^2, for 30-day back trajectories cluster of a passive air tracer, averaged over the different MOSAIC campaign seasons. The gray shading indicates the corresponding average sea-ice cover, differentiated according to regions with 30%, 50% and 99% sea-ice concentration.*

Bottom: Time series of the FLEXPART footprint emission sensitivity, integrated over the different regions shown in the map on the right. In addition, the different degrees of shading over the Arctic Ocean indicate the yearly sea ice cover, differentiated by concentration as above. The thickness of each colored layer represents the contribution of the corresponding region. The quantity in the time series is expressed in units of s m^{-1} such that, when multiplied by the emissivity flux of a species over a region (given in units of kg m^{-2} s^{-1}), it gives an estimate of the relative contribution of each region to the total concentration (in kg m^{-3}) observed at the ship position.

Summary of plans for the continuation of the project (10 lines max)

We will create a Lagrangian re-analysis with the new ERA5 dataset, similar to the already existing one. In addition, these two Lagrangian datasets (with ERA-I and ERA5) will be compared with each other and the mass distribution of the particles will be examined. This Lagrangian re-analysis will then be used for further studies on the tropical energy export on a climatological perspective. Inverse modelling will be applied to a range of different greenhouse gases (GHG) to investigate their flux changes over the last one or two decades. Furthermore, the emission sensitivity of more ice core sites will be simulated employing ERA5 data. Additionally, the ERA5 data will be used to investigate the emissions sensitivity of a Swiss tall-tower site. Finally, FLEXPART and the ERA5 dataset will be used to provide products similar to those for MOSAiC also for other measurement campaigns, such as the Atmospheric Tomography Mission (ATom).

List of publications/reports from the project with complete references

……

References:

Pisso, I. *et al.* (2019) 'The Lagrangian particle dispersion model FLEXPART version 10.4', *Geoscientific Model Development*, 12(12), pp. 4955–4997. doi: 10.5194/gmd-12-4955-2019.

Ruckstuhl, A. F. *et al.* (2012) 'Robust extraction of baseline signal of atmospheric trace species using local regression', *Atmospheric Measurement Techniques*, 5(11), pp. 2613–2624. doi: 10.5194/amt-5-2613-2012.

Stohl, A. et al. (2005) 'Technical note: The Lagrangian particle dispersion model FLEXPART version 6.2', Atmospheric Chemistry and Physics. Copernicus GmbH, 5(9), pp. 2461–2474. doi: https://doi.org/10.-5194/acp-5-2461-2005.

Stohl, A. *et al.* (2009) 'An analytical inversion method for determining regional and global emissions of greenhouse gases: Sensitivity studies and application to halocarbons', *Atmospheric Chemistry and Physics*. Copernicus GmbH, 9(5), pp. 1597–1620. doi: https://doi.org/10.5194/acp-9-1597-2009.